The Origin of the Hydration Interaction of Lipid Bilayers from MD Simulation of Dipalmitoylphosphatidylcholine Membranes in Gel and Liquid Crystalline Phases

Ulrich Essmann, Lalith Perera, and Max L. Berkowitz*

Department of Chemistry, University of North Carolina, Chapel Hill, North Carolina 27599

Received April 6, 1995. In Final Form: August 15, 1995®

The results of four molecular dynamics simulations of dipalmitoylphosphatidylcholine (DPPC)/water systems are reported. To investigate the origin of the hydration force we follow the experiments performed recently by McIntosh and Simon. We study the DPPC/water system in both the gel phase and the liquid crystalline phase at two different water contents, namely at 11 and 20.5 water molecules/lipid. Long ranged Coulomb interactions are treated with the so-called particle mesh Ewald method. The polarization profile of the water is calculated. We find that the polarization decays smoothly within 6 Å. The smoothly decaying polarization profile is a result of the roughness of the bilayer surface even in the gel phase. Furthermore we characterize the structure around the lipid head group and find a layer of water molecules with stronger hydrogen bonds. At low water contents we observe that a significant fraction of head groups of opposing bilayers is either in close contact or separated by just one or two water layers. In our interpretation, the region of water molecules with stronger hydrogen bonds keeps the opposing head group pairs separated by one or two water layers. Both situations, close contact and separation by one or two water layers, possibly give rise to the so-called hydration force.

I. Introduction

When charged or electroneutral lipid bilayers approach each other to distances of 5–15 Å one observes a strong repulsive force acting between them.[1] This force is termed the solvation (hydration) force, because, as was suggested, it is due to the solvent (usually water).[2] It was also demonstrated that a similar short range force acts between DNA molecules and polysaccharides.[3]

In spite of the rather universal appearance of this force, its nature is still not clear and is a subject of a controversy.[4–6] Some researchers ascribe the force to the ordering of solvent (water) by the surfaces of biomolecules. Such a mechanism is described by order parameter theories starting with the work of Marčelja and Radić[7] and extended by Kornyshev and Leikin[8] and Cevc.[9] A completely different explanation for the origin of the hydration force was recently given by Israelachvili and Wennerström,[10,11] who propose that the short range repulsion force is due to steric interactions of biomolecules that protrude into the fluid space. It is also possible that the repulsion force is due to both hydration and protrusion mechanisms and for some systems the hydration mechanism is dominating, while, in other systems the protrusion causes the repulsion. Such a scenario was proposed by Marrink et al.[12] and Berkowitz and Raghavan[13] (based on simulations) and by Lipowsky and Grotehans[14,15] (based on theoretical considerations of the problem).

If different mechanisms contribute simultaneously to the force, one should be able to observe different regimes of the repulsive force. Indeed, in recent measurements McIntosh and Simon found that the force decay is not described by just one exponent but by a combination of exponents, thus indicating that several mechanisms may be responsible for the nature of the short range repulsion.[16] According to McIntosh and Simon, the force between neutral membrane molecules acting at very short distances (below 4 Å) is due to very short range steric repulsion. At short distances (~4–5 to ~8–10 Å), the force arises from either the ordering of water or protrusions of lipid molecules. When the distance between fluid membranes is above 10 Å the repulsion, according to McIntosh and Simon, is due to undulation.[17] To determine the dominating mechanism of the force at distances between ~4–5 and ~8–10 Å McIntosh and Simon performed measurements on DPPC/water in the subgel phase and on egg PC/water in the liquid crystalline phase.[1] They observed that the force in this range was the same when membranes were in the subgel phase or in the liquid crystalline phase. Assuming that protrusions of molecules in the subgel phase are strongly subdued, McIntosh and Simon concluded that the force at this range is the proper hydration force, which means it is due to water orientation.

The membrane/water system has been the subject of a number of simulation studies.[12,13,18–30] (For a comprehensive survey of the simulation of lipid bilayers, see the

* Author to whom correspondence should be addressed. E-mail: maxb@gibbs.oit.unc.edu.

® Abstract published in *Advance ACS Abstracts,* November 1, 1995.

(1) McIntosh, T. J.; Simon, S. A. *Annu. Rev. Biomol. Struct.* **1994**, *23*, 27.
(2) Rand, R. P.; Parsegian, V. A. *Biochim. Biophys. Acta* **1989**, *988*, 351.
(3) Leikin, S.; Parsegian, V. A.; Rau, D. C.; Rand, R. P. *Annu. Rev. Phys. Chem.* **1993**, *44*, 369.
(4) Parsegian, V. A.; Rand, R. P. *Langmuir* **1991**, *7*, 1299.
(5) Israelachvili, J. *Langmuir* **1992**, *8*, 1501.
(6) Parsegian, V. A.; Rand, R. P. *Langmuir* **1992**, *8*, 1502.
(7) Marčelja, S.; Radić, N. *Chem. Phys. Lett.* **1976**, *42*, 129.
(8) Kornyshev, A. A.; Leikin, S. *Phys. Rev. A* **1989**, *40*, 6431.
(9) Cevc, G. *J. Chem. Soc., Faraday Trans.* **1991**, *87*, 2733.
(10) Israelachvili, J. N.; Wennerström, H. *Langmuir* **1990**, *6*, 873.
(11) Israelachvili, J. N.; Wennerström, H. *J. Phys. Chem.* **1992**, *96*, 520.
(12) Marrink, S.-J.; Berkowitz, M. L.; Berendsen, H. J. C. *Langmuir* **1993**, *9*, 3122.
(13) Berkowitz, M. L.; Raghavan, K. In *Biomembrane Electrochemistry*; Blank, M.; Vodyanoy, I., Ed.; Advances in Chemistry Series 235; American Chemical Society: Washington, DC, 1994; pp 1–25.
(14) Lipowsky, R.; Grotehans, S. *Europhys. Lett.* **1993**, *23*, 599.
(15) Lipowsky, R.; Grotehans, S. *Biophys. Chem.* **1994**, *49*, 27.
(16) McIntosh, T. J.; Simon, S. A. *Biochemistry* **1993**, *32*, 8374.
(17) Helfrich, W. *Z. Naturforsch.* **1978**, *33a*, 305.
(18) Raghavan, K.; Reddy, M. R.; Berkowitz, M. L. *Langmuir* **1992**, *8*, 233.
(19) van der Ploeg, P.; Berendsen, H. J. C. *J. Chem. Phys.* **1982**, *76*, 3271.
(20) van der Ploeg, P.; Berendsen, H. J. C. *Mol. Phys.* **1983**, *49*, 233.
(21) Scott, H. L. *Chem. Phys. Lett.* **1984**, *109*, 570.
(22) Scott, H. L. *Biochim. Biophys. Acta* **1985**, *814*, 327.
(23) Ahlström, P.; Berendsen, H. J. C. *J. Phys. Chem.* **1993**, *97*, 13691.
(24) Damodaran, K. V.; Merz, K. M. *Langmuir* **1993**, *9*, 1179.

0743-7463/95/2411-4519$09.00/0

recent review of Pastor.[31]) Our present work is a computer simulation of the McIntosh and Simon experiments. To elucidate the origin of the hydration force, we compare the structure of the lipid/water interface when the lipid is in the gel phase and in the liquid crystalline phase. Initially our intention was to perform the simulation in the subgel phase. However, as the spatial distribution of the nitrogen atoms indicates (see section III.A) we are unable to decide if the system is in the subgel or gel phase. Therefore the terms "subgel phase" and "gel phase" are used synonymously with respect to the simulated system. We perform our simulations for two different water contents. From experiments it is well-known that the maximum water content for the subgel phase of DPPC is around 11 water molecules/lipid.[32] Liquid crystalline systems, however, can adsorb more than 20 water molecules/lipid.[32,33] In a given phase, a comparison of a system at small water content with a system at larger water content should give insight into the question of how the structure of the water changes with increasing water content. This information might furthermore help to understand the underlying physical mechanism which governs the hydration of lipid membranes. Therefore, we decided to investigate the lipid/water system in the liquid crystalline state at two different water contests, at 11 and 20.5 water molecules/lipid. At a water content of 20.5 water molecules/lipid the hydration limit is not reached; however, the hydration pressure reaches only a relatively small value of 10 bar compared to several hundred bar at low water contents.[33] To investigate the differences in the hydration behavior in different phases of the lipid, we simulate the water/lipid system for these two water contents both in the liquid crystalline phase and in the subgel phase. As mentioned above the water content of 11 water molecules/lipid corresponds to the maximum hydration level of the subgel phase. The water content of 20.5 water molecules/lipid, although unphysical for the subgel phase, has two advantages: (1) a direct comparison between subgel and liquid crystalline phases is possible and (2) the increased water content can provide information as to why the extra water cannot be accommodated in the real system.

II. Technical Details

A. Preparation of the Initial Configuration. Although it would be desirable to perform the simulations at constant chemical potential, we decided in this work to perform the simulations in a constant volume ensemble since it is at the moment not feasible to perform grand canonical simulations with systems of this complexity. This requires that in order to set up a simulation, we not only had to generate the molecular configurations but also to choose the box dimensions of the simulation cell.

For the liquid crystalline systems, we used final configurations of previous simulations of Marrink et al.[12] (Note that in the case of the smaller system we had to remove 32 water molecules to bring the water content in coincidence with the maximal hydration of the subgel phase of 11 water molecules/lipid.) The value for the bilayer repeat distance of $d = 62$ Å for the system with a water fraction of $c_{H_2O} = 0.335$ (corresponding to 20.5 water molecules/lipid) reported by these authors appears to be rather high. Ruocco and Shipley[32] found for this water content at $T = 60$ °C a repeat distance of $d = 56.8$ Å. The corresponding value for the system with 11 water molecules is $d = 51.5$ Å.[32] Gawrisch et al.[33] find at $T = 50$ °C for $c_{H_2O} = 0.335$ a bilayer repeat distance of about $d = 56$ Å and for the smaller water content a repeat distance of about $d = 53$ Å. To simulate the system as closely as possible to the experimental conditions, we decided to rescale the system in the z-direction, so that the size of the unit cell in this direction was 56.8 Å for the large system and 51.5 Å for the small system. The box dimensions in the x- and y-directions and, therefore, the area per head group were adjusted in such a way that the systems have the experimentally measured density[34] of 0.98 g/cm^3. For the system with 20.5 water molecules/lipid this procedure yields an area per head group of 65.8 Å^2 and for the 11 water molecules/lipid system an area of 61.3 Å^2. The change in the bilayer repeat distance read from the data of Gawrisch et al.[33] is smaller than the change found by Ruocco and Shipley.[32] If we would accept the bilayer repeat distances read from the data of Gawrisch et al. as the input to our simulations we would obtain a larger change in the area per head group. Nevertheless our present numbers and the numbers that can be obtained from the data of Gawrisch et al. are within the range of experimentally determined values.[35] We have chosen the data of Ruocco and Shipley because their experiments were performed at 60 °C, the same temperature at which the NMR order parameters were measured.[36,37]

To generate the starting configuration for the subgel phase of the DPPC/water system, we used the observation of Ruocco and Shipley[32] that the molecular arrangement of the subgel phase of the DPPC/water system is similar to the crystal configuration of DMPC (dimyristoylphosphatidylcholine). The only difference in chemical composition between DPPC and DMPC molecules is that the DPPC molecule has two more CH_2 groups in each chain. Therefore, one can generate a "crystal-like" structure of DPPC by expanding the two chains of each molecule by two CH_2 groups. To build up the crystal, we used the coordinates of an elementary cell of DMPC obtained as a result of an energy minimization of X-ray data by Vanderkooi.[38] Replicating the elementary cell in the x- and y-directions and expanding each chain of the molecules by two CH_2 groups gave a starting configuration of the lipid molecules for the subgel phase simulation. The choice of the box lengths for the subgel phase system with 11 water molecules/lipid was based on a bilayer repeat distance of 59.4 Å at maximum hydration[16] and a density of 1.1 g/cm^3 for the subgel phase system at $T = 285$ K.[34] With the above data we obtained an area per head group of 47.4 Å^2, in good agreement with the experimental value of 45.8 Å^2 [39] and the recent value of 47.9 Å^2.[40]

The crystal configuration has an area per head group of $A = 38.82$ Å^2 and a bilayer repeat distance of $d = 59.62$ Å. To match the area per head group of the full water/lipid system in the subgel phase, we rescaled the initial crystal structure in the x- and y-directions. Rescaling in the z-direction was performed to create a spacing of about 10 Å to accommodate the water which had to be added to the system. Since the crystal structure already contained two water molecules per lipid we added 9 more water molecules/lipid. These additional water molecules were taken from a liquid water simulation. The configuration composed in this way contained extra energy due to the artificial way of obtaining it which had to be removed in several stages. The first stage was an energy minimization with fixed lipid molecules. In a second stage the energy was minimized with both water and lipids moving. Finally a sequence of short MD runs was performed. At the end of each run, the velocity information was discarded. This procedure removed the remaining excess energy and completed the preparation process.

(25) Egberts, E.; Marrink, S.-J.; Berendsen, H. J. C. *Eur. Biophys. J.* **1994**, *22*, 423.
(26) Marrink, S.-J.; Berendsen, H. J. C. *J. Phys. Chem.* **1994**, *98*, 4155.
(27) Damodaran, K. V.; Merz, K. M. *Biophys. J.* **1994**, *66*, 1076.
(28) Wilson, M. A.; Pohorille, A. *J. Am. Chem. Soc.* **1994**, *116*, 1490.
(29) Heller, H.; Schaefer, M.; Schulten, K. *J. Phys. Chem.* **1993**, *97*, 8343.
(30) Zhou, F.; Schulten, K. *J. Phys. Chem.* **1995**, *99*, 2194.
(31) Pastor, R. W. *Current Opin. Struct. Biol.* **1994**, *4*, 486.
(32) Ruocco, M. J.; Shipley, G. G. *Biochim. Biophys. Acta* **1982**, *691*, 309.
(33) Gawrisch, K.; Ruston, D.; Zimmerberg, J.; Parsegian, V. A.; Rand, R. P.; Fuller, N. *Biophys. J.* **1992**, *61*, 1213.
(34) Tristram-Nagle, S.; Wiener, M. C.; Yang, C.-P.; Nagle, J. F. *Biochemistry* **1987**, *26*, 4288.
(35) Nagle, J. F. *Biophys. J.* **1993**, *64*, 1476.
(36) Seelig, A.; Seelig, J. *Biochemistry* **1974**, *13*, 4839.
(37) Seelig, A.; Seelig, J. *Biochemistry* **1977**, *16*, 45.
(38) Vanderkooi, G. *Biochemistry* **1991**, *30*, 10760.
(39) Church, S. E.; Griffiths, D. J.; Lewis, R. N. A. H.; Wickman, H. *Biophys. J.* **1986**, *49*, 597.
(40) Sun, W. J.; Suter, R. M.; Knewton, M. A.; Worthington, C. R.; Tristram-Nagle, S.; Zhang, R.; Nagle, J. F. *Phys. Rev. E* **1994**, *49*, 4665.

Table 1. Conditions of the Four Simulations

no.	description	area/head group, Å^2	repeat distance, Å	water space, Å	density, g/cm^3	water/lipid	T, K
1	small gel	47.4	59.4	9.0	1.10	11	285
2	large gel	47.4	71.4	20.7	1.08	20.5	285
3	small liq cryst	61.3	51.5	4.9	0.98	11	333
4	large liq cryst	65.8	56.8	12.1	0.98	20.5	333

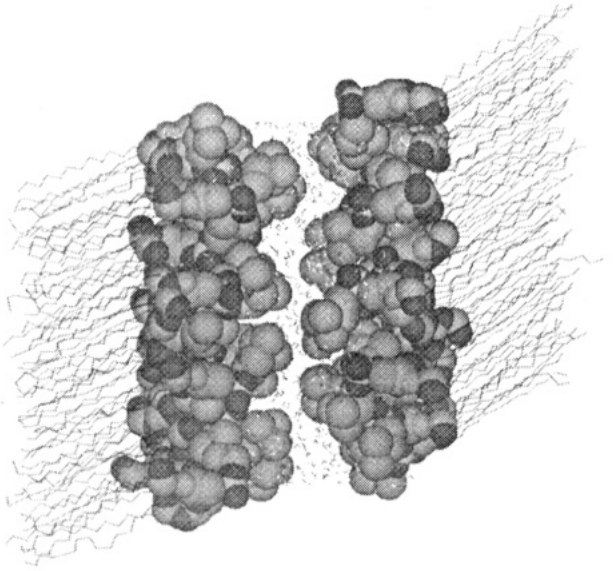

Figure 1. Snapshot of the small gel phase system. The water molecules are in the middle. The head group atoms are represented by spheres. The hydrophobic chains are in stick representation on the left and right sides of the picture.

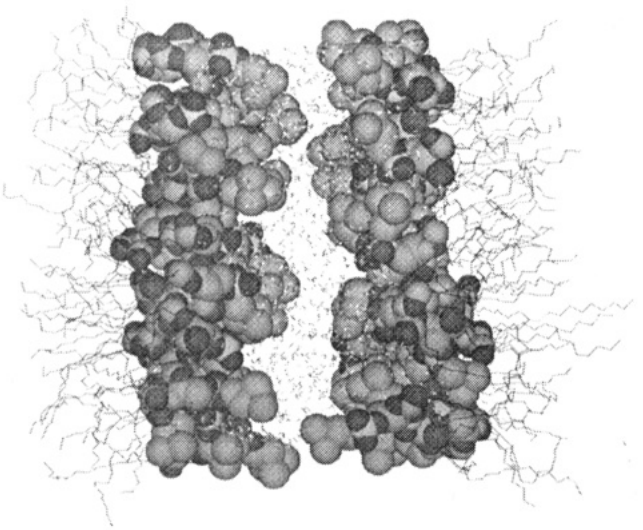

Figure 2. Snapshot of the large liquid crystalline system. The representation is the same as for the gel phase system.

The subgel phase system with 20.5 water molecules/lipid was set up so that it had the same area per head group as the smaller subgel phase system. The bilayer repeat distance was increased so that the additional volume corresponds to adding 9.5 water molecules/lipid at a density of 1 g/cm^3. This led to a repeat distance of 71.4 Å. The preparation followed closely the procedure described above for the smaller subgel phase system.

To summarize, we simulated four systems, two in the subgel phase and two in the liquid crystalline phase. Each of the four systems consisted of 64 lipid molecules plus the appropriate number of water molecules (1315 water molecules for the larger systems and 704 water molecules for the smaller systems). The conditions for the four simulations are given in Table 1. In Figure 1 we display a snapshot of the small gel phase system and in Figure 2 a snapshot of the large liquid crystalline system.

B. Algorithm. We used a modified version of the standard program AMBER 3a [41] for our simulations. In this version all calculations were done in exactly the same way as in the standard version, except the calculation of the nonbonded interaction.

As has been shown in previous studies, the correct treatment of the long range Coulomb interaction is important.[30,42,43] For the calculation of the Coulomb interactions the recently invented particle mesh Ewald (PME) method of Darden et al.[44] was used. This method combines the particle−particle mesh approach of Hockney and Eastwood[45] with the traditional Ewald summation. In the PME approach, the total Coulomb interaction is divided into a short ranged "direct" part and a long ranged "reciprocal" part. The direct part allows a cutoff radius beyond which the interactions can be neglected. The reciprocal part is approximated on a grid thereby allowing the use of fast Fourier transformations. It has been shown[44] that this method gives, even for moderate grid sizes (spacing of the grid 0.75−1 Å), an accuracy of 10^{-5}−10^{-6} for the calculated Coulomb interactions.

For the representation of the molecules, we used the united atom approach. All parameters including the parameters for the water molecules were taken from STUB section of the PARM91 file[46] except for the alkane chains of the lipid tails. Following the approach of Egberts and Berendsen,[47] we represented the intramolecular 1−4 interactions within alkane chains by the Ryckaert−Bellemans potential.[48,49]

All intramolecular bond lengths within the lipid molecules were fixed with the SHAKE algorithm.[50] The simulations were performed in the constant volume ensemble. We studied the subgel phase systems at $T = 285$ K and the two liquid crystalline phase systems at $T = 333$ K. The temperature of the water, as well as the temperature of the lipid molecules, was coupled separately to an external heat bath with a time constant of 0.2 ps. The time step was 2 fs. The length of each run was 300 ps after equilibration. Averages were calculated from the last 200 ps. The neighbor lists were updated at every fifth step.

C. Derivation of Charges. In the previous calculations from our group,[18] the partial atomic charges were calculated using the Gaussian 86 program at the 3-21G* basis set level and the CHELP module.[51] The whole lipid molecule was divided into two fragments, the head group, including the glycerol group, and the tail atoms. Presently, we reevaluated the partial atomic charges. The whole head group including the carbonyl group was taken as one fragment. We selected 32 different lipid configurations from previous membrane simulations.[12] Since it is not feasible to perform the calculations for all the 32 configurations at the 6-31G** level, we used the method described by Chirlian and Francl.[51] They suggested that a linear correction can be applied to scale the partial charges obtained from the 3-21G* basis set to match those of the 6-31G*. First we evaluated the charges at the 3-21G* basis set level using Gaussian 92

(41) Singh, U. C.; Weiner, P. K.; Caldwell, J. W.; Kollman, P. A. *AMBER (Version 3.1)*, Department of Pharmaceutical Chemistry, University of California, San Francisco, 1988.
(42) York, D. M.; Darden, T. A.; Pedersen, L. G. *J. Chem. Phys.* **1993**, *99*, 8345.
(43) Alper, H. E.; Bassolino, D.; Stouch, T. R. *J. Chem. Phys.* **1993**, *98*, 9798.
(44) Darden, T.; York, D.; Pedersen, L. *J. Chem. Phys.* **1993**, *98*, 10089.
(45) Hockney, R. W.; Eastwood, J. W. *Computer Simulation using Particles*; McGraw-Hill: New York, 1981.
(46) Pearlman, D. A.; Case, D. A.; Caldwell, J. C.; Seibel, G. L.; Singh, U. C.; Weiner, P.; Kollman, P. A. AMBER (Version 4.0), University of California, San Francisco, 1991.
(47) Egberts, E.; Berendsen, H. J. C. *J. Chem. Phys.* **1988**, *89*, 3718.
(48) Ryckaert, J.-P.; Bellemans, A. *Chem. Phys. Lett.* **1975**, *30*, 123.
(49) Ryckaert, J.-P.; Bellemans, A. *Faraday Discuss. Chem. Soc.* **1978**, *66*, 95.
(50) Ryckaert, J.-P.; Ciccotti, G.; Berendsen, H. J. C. *Comput. Phys.* **1977**, *23*, 327.
(51) Chirlian, L. E.; Francl, M. M. *J. Comput. Chem.* **1987**, *8*, 894.

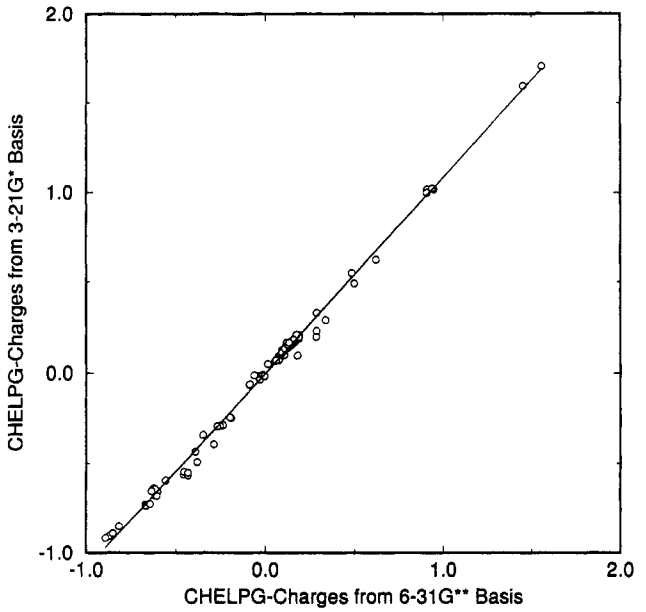

Figure 3. Plot of the charges calculated for two lipid configurations with the 3-21G* basis set versus corresponding charges calculated for the same configurations using the 6-31G** basis set. All calculations were done with Gaussian92. The charges were fitted with the CHELPG module.

Table 2. Charges of DPPC. For the Nomenclature of the Atoms See Figure 4

atom	charge	atom	charge
C13	0.155	O21	−0.535
C14	0.155	C21	0.826
C15	0.155	O22	−0.586
N	0.221	C22	0.000
C12	0.033		
C11	0.366	C216	0.000
O12	−0.561	C3	0.290
O13	−0.812	O31	−0.535
O14	−0.812	C31	0.826
P	1.483	O32	−0.586
O11	−0.561	C32	0.000
C1	0.198		
C2	0.279	C316	0.000

program and the CHELPG module.[52] For only 2 of the 32 configurations we calculated the charges with the 6-31G** basis set. Indeed, the plot of the 3-21G* charges calculated for the 2 selected configurations versus their corresponding 6-31G** values shows a linear relationship with a slope of 1.084 959 and an intercept of 8.755 126 × 10^{-7} (see Figure 3).

Finally, the values of the partial charges were adjusted to reflect symmetries within the molecular structure. For example, the three values for the CH_3 groups of the $N(CH_3)_3$ group were set to their average value. The partial charges for the alkane chain atoms of the tails were set to zero. The final atomic charges are tabulated in Table 2. Figure 4 shows the nomenclature for the atomic positions within the molecule.

III. Results

A. Spatial Structure of the Systems. One way of characterizing the structure of the water/membrane interface is to calculate the distribution of the atoms as a function of a coordinate perpendicular to the bilayer (called the *z*-direction). The position of the head group is characterized by the distribution of the nitrogen atoms

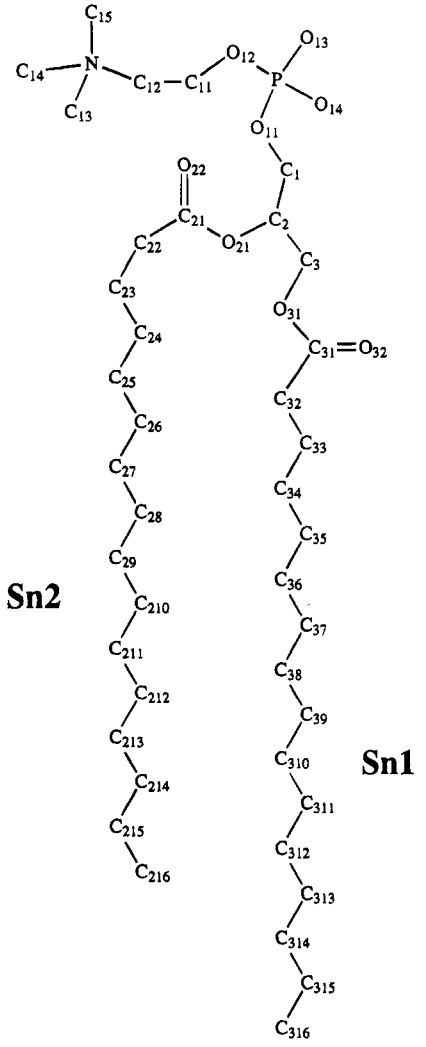

Figure 4. Nomenclature of the atoms in the DPPC molecule.

and their methyl groups and by the position of the phosphorus atoms. The distribution of the carbonyl groups, however, indicates the locations of the centers of mass of the molecules since they are located close to them. In the top panel of Figures 5a−8a, all the above-mentioned distributions for the four systems are plotted allowing a better comparison of the relative locations of the different groups. In the three other panels the particularly interesting distributions for water, phosphorus, and nitrogen are plotted separately.

An important parameter for the characterization of the multilayer system is the thickness of the fluid space between the bilayers. However, as can be seen in Figures 5b−8b the location of the boundaries of the fluid space is rather arbitrary. In some of the experiments electron density profiles have been used to define this boundary.[53] Since the maximum of the electron density profile is close to the location of the phosphorus groups and the lipid extends for about another 5 Å into the water layer, a plane 5 Å away from the electron maximum has been defined as the edge of the bilayer.[53] The boundaries have been determined from Figures 9 and 10 and are indicated as dotted lines in Figures 5−8.

A comparison of the subgel phase systems (Figures 5 and 6) with the liquid crystalline systems (Figures 7 and 8) shows that peaks for the individual groups are much better developed in the gel phase than in the liquid crystalline phase, reflecting the higher degree of order in

(52) Frisch, M. J.; Trucks, G. W.; Head-Gordon, M.; Gill, P. M. W.; Wong, M. W.; Foresman, J. B.; Johnson, B. G.; Schlegel, H. B.; Robb, M. A.; Replogle, E. S.; Gomperts, R.; Andres, J. L.; Raghavachari, K.; Binkley, J. S.; Gonzalez, C.; Martin, R. L.; Fox, D. J.; Defrees, D. J.; Baker, J.; Stewart, J. J. P.; Pople, J. A. *Gaussian 92, Revision E.2*; Gaussian Inc.: Pittsburgh, PA, 1992.

(53) McIntosh, T. J.; Simon, S. A. *Biochemistry* **1986**, *25*, 4058.

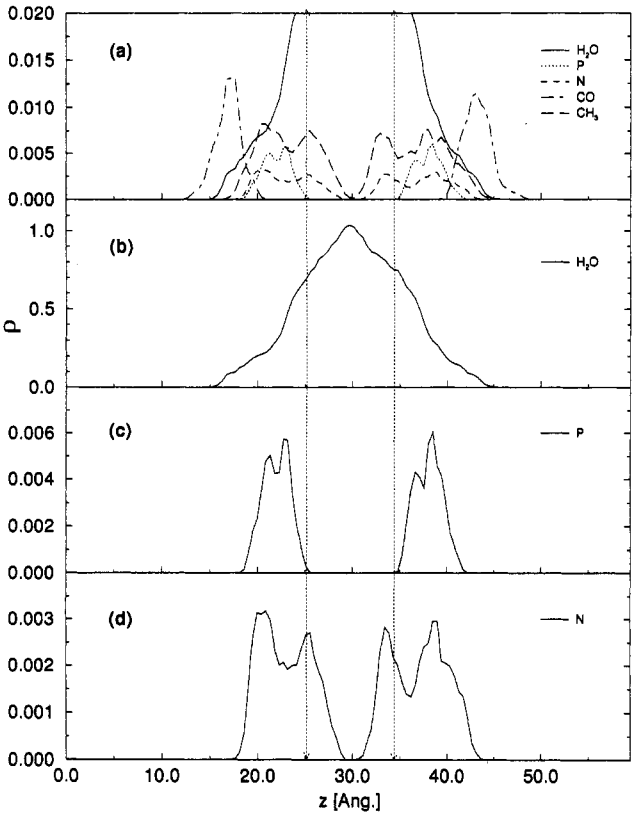

Figure 5. Small gel phase simulation: distributions of atoms along the z-axis, perpendicular to the bilayer surface. Note that we display only the distribution of CH_3 groups attached to the nitrogen atom of the head group. The dotted vertical arrows indicate the boundary between lipid and water as defined in the text. The y-axis of all panels is in molecules/Å^3 (or groups/Å^3), except panel b which is in g/cm^3.

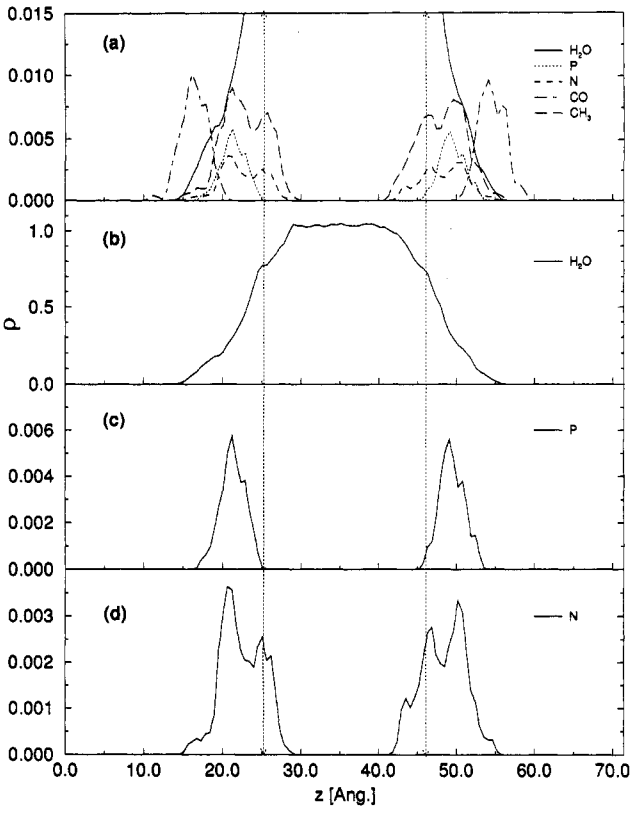

Figure 6. Large gel phase simulation: distributions of atoms along the z-axis. The notation is the same as in Figure 5.

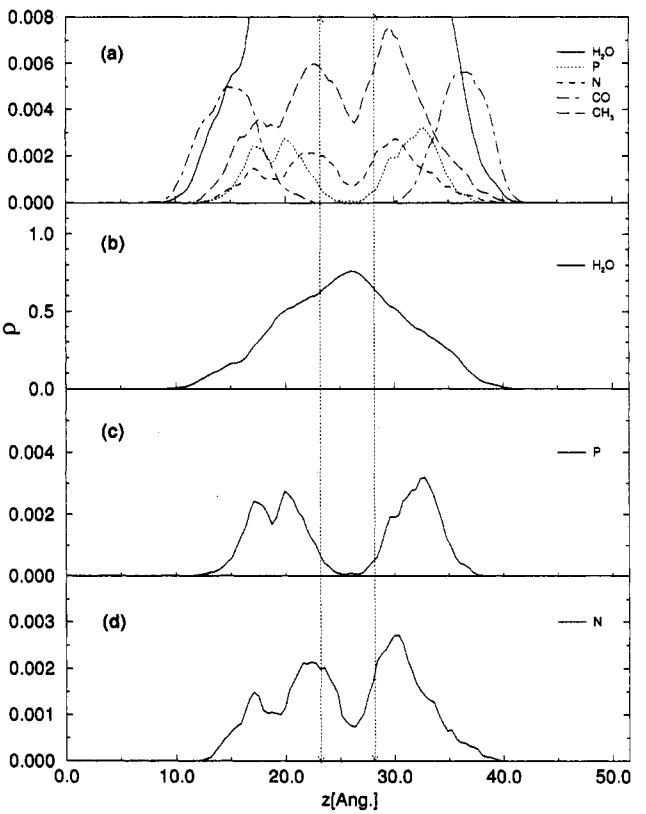

Figure 7. Small liquid crystalline phase simulation: distributions of atoms along the z-axis. The notation is the same as in Figure 5.

the gel phase. (Differences appearing between the left and right sides of the bilayer as, for example, in the phosphorus distribution of the large liquid crystalline system (Figure 8), are a consequence of the slow relaxation of the system. It gives some idea of the "error" in the distribution functions.)

The distribution for the carbonyl groups, for example, has in the subgel phase a width of about 2−3.5 Å while it has a width of 6.5−7.5 Å in the liquid crystalline system. The width of the distribution increases in all systems toward the head. The surprising fact is that the width of the nitrogen distribution in the gel phase is rather large. While the width of the distribution of phosphorus is about 3.5−4 Å, the corresponding value for the nitrogen distribution is between 6.5 and 8 Å. The double peak form of the nitrogen distributions suggests that the head groups arrange in two different conformations.

We confirmed this hypothesis by dividing the nitrogen distribution into two distributions separated by the minima of the distribution function. This division was done after 100 ps of the simulation run. After another 200 ps we find that all the nitrogens stayed in their subregions. We observe that the head groups remained during the simulations in two distinct conformations thereby forming a rather rough surface. The two conformations are already present in the crystal structure of DMPC from which the initial configuration for our simulation was obtained (see Figure 6 of ref 54) and the energy minimized structure in Figure 2 of ref 38. The nitrogen atoms of the two conformations have a separation in the z-direction of about 4.3 Å in the data set of Vanderkooi.[38] The roughness of the surface formed by the head groups in the gel phase is also reflected in the distribution of the water molecules. Rather than forming a sharp boundary, the density of the water drops continu-

(54) Hauser, H.; Pascher, I.; Pearson, R. H.; Sundell, S. *Biochim. Biophys. Acta* **1981**, *650*, 21.

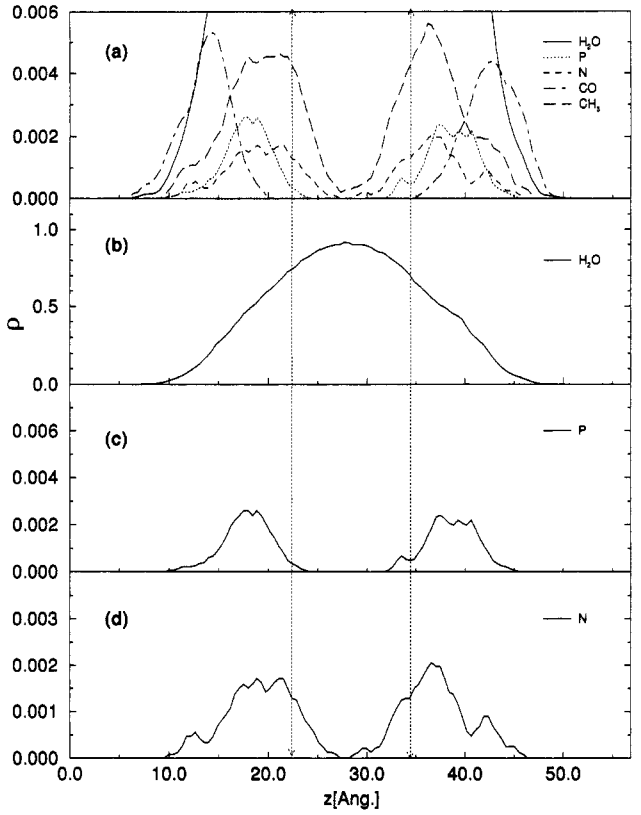

Figure 8. Large liquid crystalline phase simulation: Distributions of atoms along the z-axis. The notation is the same as in Figure 5.

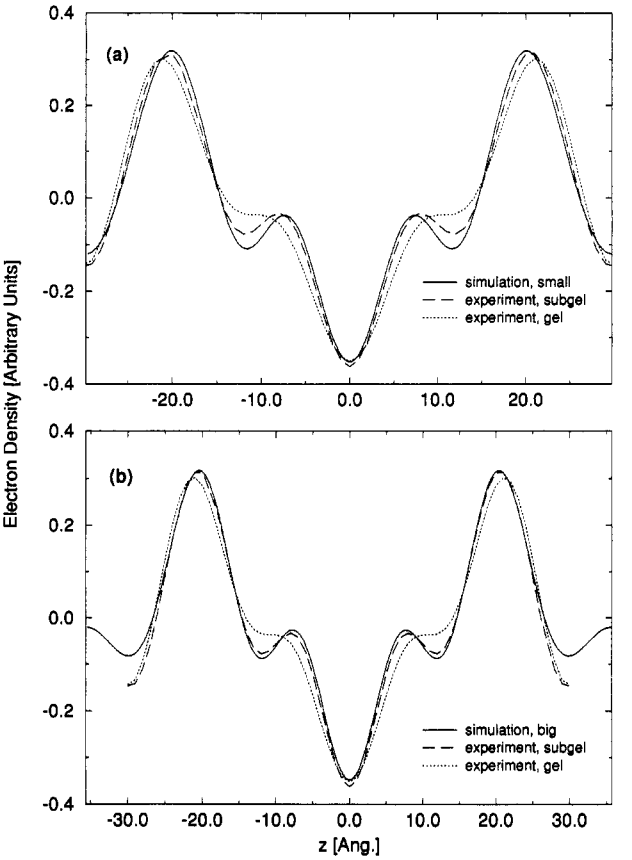

Figure 9. Electron density profiles. Comparison between electron density profiles from simulations in the gel phase and experiments. The experimental data were obtained from subgel and gel phase systems at $T = 283$ and 293 K, respectively.

ously. One way of quantifying the width of the boundary is by measuring the distance in which this density drops from 90% to 10% of the maximal value. For the small and the large gel phase systems we obtained values of 10.6 and 10.2 Å and for the case of the small and large liquid crystalline systems, values of 10.9 and 12.2 Å.

In the center of the fluid space, the water density in both gel phase systems reaches a value of 1.03−1.05 g/cm^3. The density of the water in the small liquid crystalline system reaches a value of only 0.76 g/cm^3 and in the large liquid crystalline system a value of 0.95 g/cm^3. However, it is misleading to conclude from this fact that the local density of the water in the middle of the system is lower than 1.0 g/cm^3 since we calculated the average density in slabs parallel to the bilayer surface. The nonzero densities for the methyl groups and nitrogen atoms in the center of the system reduce considerably the accessible volume for the water molecules in this region, thereby reducing the number of molecules in the slabs.

Finally we found that water molecules penetrate into lipid region up to the carbonyl group; a result consistent with previous simulations[12] and experiments.[1,55] The penetration in the gel phase is slightly smaller than that in the liquid crystalline phase probably due to the smaller area per head group.

In view of the broad distribution of the nitrogen atoms, it is difficult to judge if the system is in the subgel or the gel phase. Even though we choose the parameters so that they match the subgel phase values there is a chance that during the preparation process the system went into the gel state. Since the precise structure in the subgel phase is not known, we are not able to distinguish between the two states. Therefore, we refer in the following to these systems in a generic way as being in the "gel phase", thereby leaving the question of whether they are indeed in the gel phase or the subgel phase open.

B. Electron Density Profile. The electron density profile has been determined by X-ray scattering. For the calculation of the electron density profiles from simulations, the nuclear charges on individual atoms were corrected by the partial charges used in the simulation and listed in Table 2. For a comparison with experimental data one has to keep in mind that the experimental electron density profile is usually recorded with a resolution of 3.5−7 Å [16] and, therefore, many features are not as pronounced as in the simulated profiles. In X-ray experiments the so-called structure amplitude $F(h)$ is calculated from the measured integrated intensities $I(h)$ according to $F(h) = \{hI(h)\}^{1/2}$ for each diffraction order h.[16] From the structure amplitude $F(h)$ the electron density profiles $\rho(z)$ are calculated by Fourier transformation:

$$\rho(z) = (2/d)\sum_h \exp\{i\phi(h)\}F(h)\cos(2\pi zh/d) \quad (3.1)$$

where d is the bilayer repeat distance and $\phi(h)$ the phase angle for the order h. For symmetric bilayers the phase factors $\exp(i\phi(h))$ has values of ± 1.[56] In the simulations the electron density profiles are first calculated from the total charges and positions of the atoms. The structure amplitudes are then calculated from these profiles by Fourier transformation, and therefore all the phase factors are known. In experiments only structure amplitudes up to a maximum value h_{max} are used for the Fourier synthesis

(55) Wong, P. T. T.; Mantsch, H. H. *Chem. Phys. Lipids* **1988**, *46*, 213.

(56) Worthington, C. R.; King, G. I.; McIntosh, T. J. *Biophys. J.* **1973**, *13*, 480.

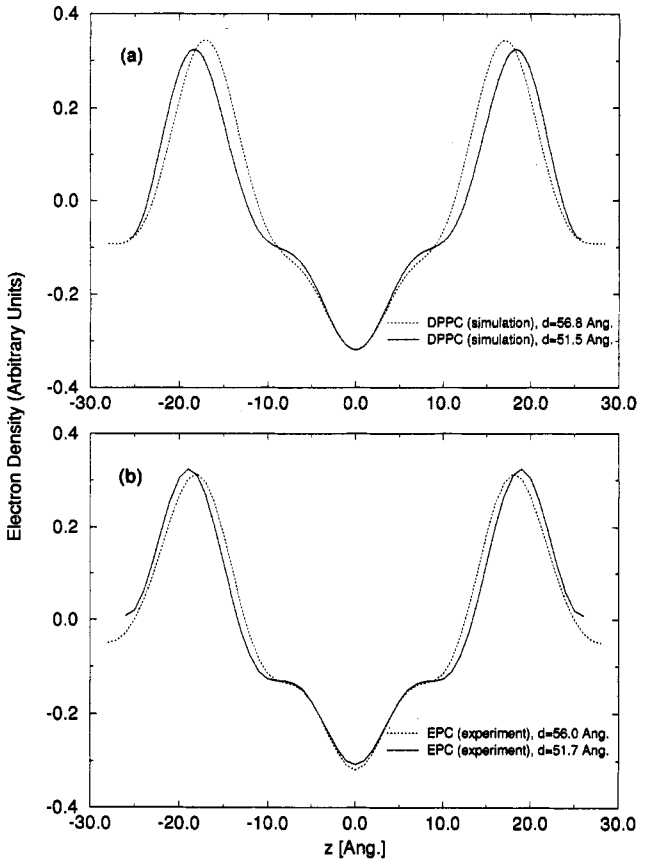

Figure 10. Electron density profiles: (a) small and large liquid crystalline systems from simulation and (b) experimental data for egg PC at $T = 293$ K for similar repeat distances as in the simulation.

of the electron density profiles. McIntosh and Simon used in their experiments[16] resolutions of $d/2h_{max} \approx 7$ Å and $d/2h_{max} \approx 3.5$ Å. To compare the electron density profiles from simulation with experiments we use for the Fourier synthesis of the final electron density profiles only structure amplitudes up to the above-mentioned values of h_{max}.

The resulting data for the gel phase systems are shown in Figure 9 along with experimental curves for gel and subgel phase systems. From experiment we know that the bilayer thickness is only weakly dependent on the water content.[16] This allows us to compare the data of the small as well as the large gel phase simulation with the experimental data. The data for the liquid crystalline systems are compared with that of egg PC (EPC) in Figure 10. The temperature of the EPC systems in the experiment was about 18 °C above the gel–liquid crystalline phase transition. In our simulations the temperature of the DPPC systems was also about 18 °C above the gel–liquid crystalline transition. In Figures 9 and 10 the center of the bilayer is in the middle of the graph to make the comparison between experimental and simulated data easier. The data from the simulation reproduce well the minimum in the electron density in the center of the bilayer. A comparison with Figures 5–8 shows that the maximum of the electron density is close to the maximum of the phosphorus distribution, even though it is slightly shifted toward the membrane interior.

The agreement between simulated and experimental electron density profiles for the gel phase systems is very good. The electron density profiles have been used to define the boundaries between the bilayer and the water. As mentioned in section III.A, McIntosh and Simon[53] defined it as the plane 5 Å away from the maximum of the electron density profile into the water. As can be seen in Figure 9 the thickness of the bilayer in the gel phase simulation is close to the corresponding experimental values of the gel and subgel phase systems. The peak-to-peak distances for the small and large simulated systems are 40.4 and 40.7 Å, respectively (bilayer thicknesses of 50.4 and 50.7 Å). For comparison the value for the peak-to-peak distances[16] for the subgel phase is 41 Å and that for the gel phase is 41.9 Å. The simulated data are closer to the subgel phase value, and the overall shape of the electron density profiles is closer to that of the subgel phase experiment. However, since the experimental gel and subgel phase values are very close to each other it is difficult to make a definitive statement.

The comparison between the simulated liquid crystalline data of DPPC with experimental data for EPC shows that the bilayer thickness of the DPPC system is consistently 1.4 Å smaller. We find for the small simulated system a peak-to-peak distance of 36.6 Å and for the large simulated system 34.7 Å (bilayer thicknesses of 46.6 and 44.7 Å). The corresponding peak-to-peak distances for the EPC systems are 38.0 and 36.0 Å. Note that for the simulated systems as well as for the experimental systems we find that the bilayer thickness increases with decreasing water content, an effect previously noticed by Torbet and Wilkins.[57] The decreased area per head group leads apparently to an expansion of the bilayer thickness. For the simulated systems we find an increase of 1.9 Å and for the experimental systems an increase of 2 Å.

C. Orientation of the Head Group. Since the head group of DPPC is a zwitterion, the behavior of the water/membrane system is strongly influenced by the relative orientation of the head group with respect to the bilayer normal. It is characterized by the cosine of the angle θ between the PN vector, pointing from the location of the phosphorus atom to the location of the nitrogen atom, and the unit vector along the positive z-direction. The probability distributions $P(\cos(\theta))$ for the four systems are displayed in Figure 11. In all four systems we find a very broad distribution of angles which may be especially surprising for the gel phase systems. But, as we already concluded from the distribution functions of the nitrogen atoms in Figures 5 and 6 these distributions are rather broad, due to two different conformations of the head groups. The broad distribution of nitrogen atoms gives rise to a broad distribution of PN vectors. The distribution functions in Figure 11 show no significant differences between the gel and liquid crystalline phases. (We interpret the differences between the graphs as insignificant since we find anyway rather large differences between the left and right sides of the systems.) For the average angle with respect to the bilayer normal we find a value of 77.8° for the small gel phase system and a value of 76.3° for the large gel phase system. The corresponding values for the liquid crystalline system are 75.2° and 72.2°.

D. Conformation of the Lipid Tails. The order parameter provides important insight into the conformation of the chains. It has been measured for DPPC molecules at 333 K by Seelig and Seelig.[36,37] (Actually, the order parameter was measured for the Sn1 chain.[58]) However, except for carbon atom 2 (carbon atoms C22 and C32), the differences in the order parameter between the two chains are not large.[36]) Since in our simulation the molecules are represented by a united atom approach the hydrogen positions are not available. Therefore, we adopt here a procedure described by Egberts et al.[25] The resulting S_{CD} order parameters for both liquid crystalline

(57) Torbet, J.; Wilkins, M. H. F. *J. Theor. Biol.* **1976**, *62*, 447.
(58) Seelig, J.; Browning, J. L. *FEBS Lett.* **1978**, *92*, 41.

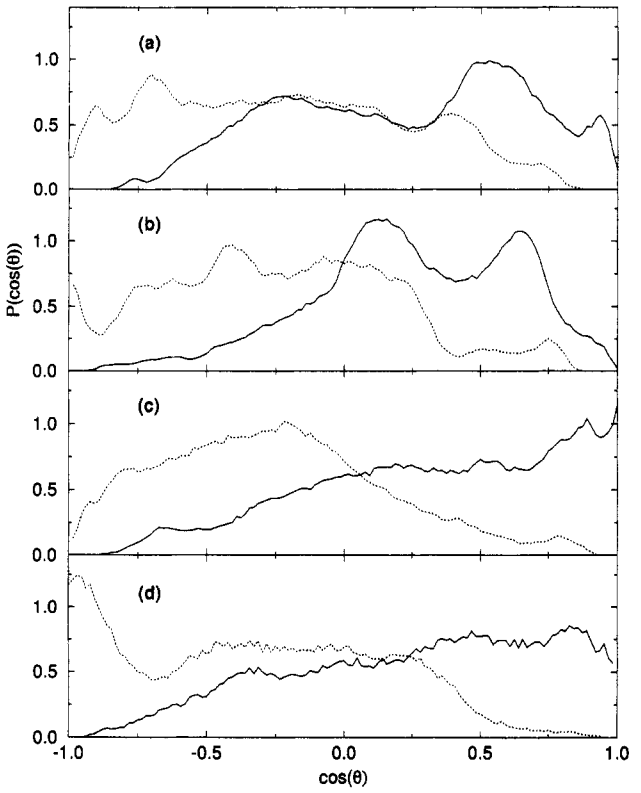

Figure 11. Distributions of cosines of the angle between the PN vector of the head group and the positive z-axis. Dotted and full lines are for the two monolayers of the system: (a) small gel phase systems, (b) large gel phase system, (c) small liquid crystalline phase system, and (d) large liquid crystalline phase system.

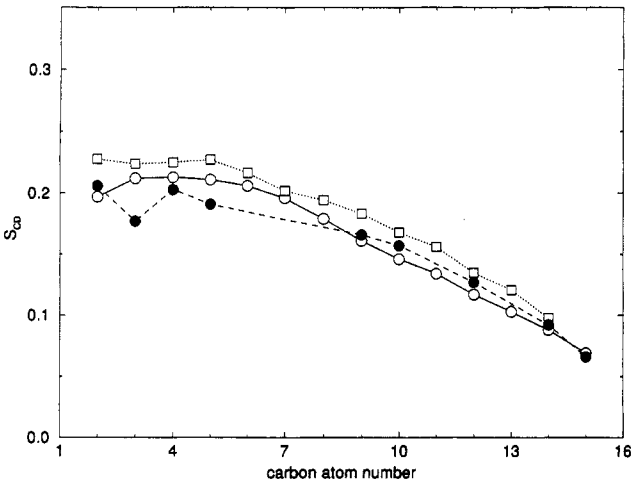

Figure 12. Order parameters for the liquid crystalline phase: (●) experimental data at $T = 333$ K, (□) data from the small liquid crystalline simulation, and (○) data from the large liquid crystalline simulation.

systems together with the experimental values for the 333K DPPC system are displayed in Figure 12. The calculated order parameters of the DPPC systems show good agreement with experiments.

The conformation of the hydrophobic tails has also been characterized by the number of gauche and trans conformations. The trans conformation can be defined in the following way: label four consecutive carbon atoms 1, 2, 3, and 4. Let us call the projections of the bond between carbon atoms 1 and 2 on a plane perpendicular to the bond between 2 and 3 vector $\vec{a}$ and similarly the projection of the bond between carbon atom 3 and 4 onto the same plane, vector $\vec{b}$. If the angle between vectors $\vec{a}$ and $\vec{b}$ is between 120° and 240°, the conformation is called trans (t). If the angle is either smaller than 120° or greater than 240° it is called gauche (g) and gauche′ (g'), respectively. Of particular importance are the gtg' conformations (kinks), the gg conformations (double gauche), and the sum of the gtg and gtg' conformations. The occurrences of different conformations per chain for the two liquid crystalline systems are listed in Table 3. The values found here are consistently lower than the experimental data. A similar observation has been made by Chiu et al.[59] in a simulation of a DMPC bilayer. However, the experimental values are quite sensitive to the details of the data analysis.[60] Note that despite the differences in the conformation statistics between experimental and simulation data, we observe that the calculated S_{CD} order parameter is in good agreement with experiments.

Table 3. Gauche/Trans Conformations in the Liquid Crystalline Systems

	small system ($T = 333$ K)	large system ($T = 333$ K)	experiment
g/chain	3.10	3.10	3.6,[a] 3.8,[b] 3.4–3.9[c]
end g/chain	0.30	0.30	0.4,[a] 0.38[c]
gg/chain	0.28	0.27	0.4,[a] 0.57[c]
gtg'/chain	0.49	0.46	
($gtg + gtg'$)/chain	0.83	0.82	0.47,[c] 1.0[a]

[a] See ref 72 at $T = 318$ K. [b] See ref 73 at $T = 315$ K. [c] See ref 60 at $T = 342$ K.

For the gel phase system we calculate the average tilt angle of the chain. We find an average angle of 33.4° for the chain tilt of the small system and an average angle of 32.2° for the large system. We note, however, that the two monolayers are tilted in different directions. At this point we are unable to decide if this is an artifact of our simulation. The tilt angle agrees reasonably well with the experimental values for the subgel phase of 29°[39] and 34.7°[61] and with the value for the gel phase of 32°.[40]

E. Structure of Water around the Lipid Head Group. According to the Marčelja–Radić theory,[7] the hydration force is caused by the structuring of water between the membranes. Therefore, we investigated the structure and energetics of the water next to the lipid head group. In this regard the simulations of Damodaran and Merz[24] revealed that the water orients around the $N(CH_3)_3$ group in DMPC in a similar way as it does around hydrophobic particles and creates "clathrate like" structures.

To assess if this behavior is independent of the phase of the bilayer, we first calculated the pair distribution function of the water molecules around the CH_3 groups and around the N atom of the DPPC head groups. The result for all four systems is displayed in Figure 13. The hydration behavior of the $N(CH_3)_3$ group as seen from the pair distribution is independent of the phase of the DPPC bilayer. We find that the distance from the N atom to the first peak of the O atom is almost the same as that to the first peak of the H atom, in agreement with Damodaran and Merz.[24] A similar effect has been observed in the simulation of neutral (hydrophobic) and slightly charged Lennard-Jones atoms[62,63] and has been interpreted as a sign of a structure promotion of the hydrogen bond network

(59) Chiu, S.-W.; Clark, M.; Balaji, V.; Subramaniam, S.; Scott, H. L.; Jakobsson, E. *Biophys. J.* **1995**, *69*, 1230.
(60) Tuchtenhagen, J.; Ziegler, W.; Blume, A. *Eur. Biophys. J.* **1994**, *23*, 323.
(61) Katsaras, J. *J. Phys. Chem.* **1995**, *99*, 4141.
(62) Geiger, A.; Rahman, A.; Stillinger, F. H. *J. Chem. Phys.* **1979**, *70*, 263.
(63) Geiger, A. *Ber. Bunsen-Ges. Phys. Chem.* **1981**, *85*, 52.

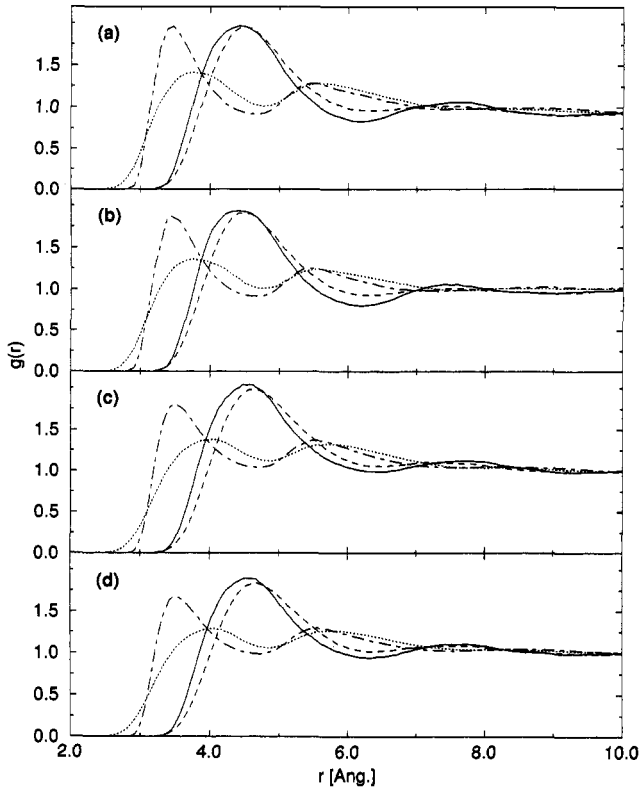

Figure 13. Pair distribution functions between head group atoms and water molecules: (i) N–O (full line), (ii) N–H (dashed line), (iii) CH_3–O (dotted–dashed line), and (iv) CH_3–H (dotted line) for (a) small gel phase system, (b) large gel phase system, (c) small liquid crystalline phase system, and (d) large liquid crystalline phase system.

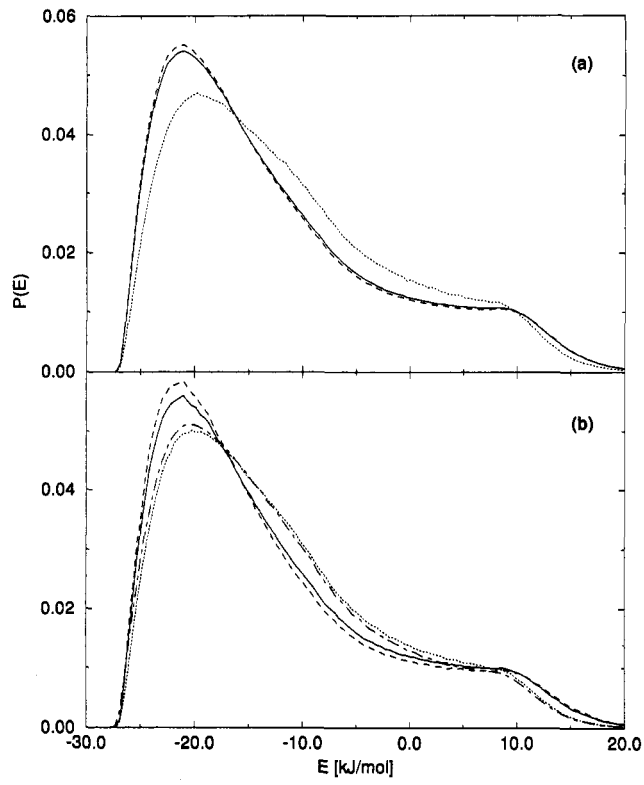

Figure 14. Distributions of pair energies: (i) full line, one molecule belongs to the first shell; (ii) dotted line, one molecule belongs to the second shell; and (iii) dashed line, both molecules belong to the first shell for (a) small subgel phase system and (b) large subgel phase system. For comparison, the distribution for a bulk system at $T = 285$ K is drawn in part b (dotted–dashed line).

close to the hydrophobic particle. The water molecules are able to form hydrogen bonds with each other by creating a "clathrate like" structure around the head group. These structures will be more distorted in this case since the head groups are connected on one side with the rest of the molecule. To investigate this topic further, we defined all water molecules with a nitrogen–oxygen distance of less than 6.4 Å (the first minimum in the N–O pair distribution functions) as belonging to the first hydration shell of the head group (see Figure 13). To confirm the observation that the hydration of the head groups is similar to the case hydrophobic hydration, we calculated the cosines of the angles between the vectors connecting the N atom and the O atom of the water molecules and either the dipole vectors $\vec{\mu}_{H_2O}$ of the water molecules or the OH vectors within the water molecules (not shown). The distribution functions are similar to the distribution functions of a neutral Lennard-Jones sphere rather than the weakly charged ions even though our distribution functions are less pronounced.[62] This observation is probably due to the fact that the positive charge is distributed over many atoms leading to a small charge density.

From the pair distribution functions in Figure 13, we also observe that the most probable distance between the CH_3 group and the first water layer is about 3.4 Å (the first maximum in the CH_3–O pair distribution functions) and the distance between the N atom and the first water layer is about 4.5 Å (the first maximum in the N–O pair distribution functions). Therefore, if two head groups approach each other, but still keep one water layer between them, the minimum distance between two CH_3 groups will be about 6.8 Å and between two N atoms 9 Å. This observation will be discussed in section III.H.

The hydrophobic hydration of the $N(CH_3)_3$ group also has important consequences for the energetics of the water molecule as can be seen from Figure 14 and 15. Here we plotted the distribution of the energies between pairs of water molecules with O–O distances less 3.6 Å. We distinguish three classes depending on their environment: (1) one of the two molecules belongs to the first hydration shell, (ii) one of the two molecules belongs to the second hydration shell, and (iii) both molecules belong to the first hydration shell. The three classes are displayed for the four systems. In all four systems we find the same trend: the pair energies are shifted to lower energies if one of the partners belongs to the first shell rather than if one of the partners belongs to the second shell. This trend is even stronger if both partners belong to the first shell. The distribution of the pair energies in the second shell, however, approaches the distribution of bulk water (see Figures 14b and 15b). Therefore, we conclude that a distinct layer of water molecules with an enhanced hydrogen bond network exists around the head groups.

We emphasize, however, that the effect of stronger hydrogen bonds around the head groups does not necessarily lead to hydration pressure between opposing membranes. The appropriate thermodynamic potential from which the hydration pressure can be calculated is the free energy. The free energy, however, has two contributions: one is energetic, and the other is entropic. The hydrogen bond energies are only a part of the energetic contribution to the free energy but can easily be outweighed by the entropic term. The free energies involved in the hydration pressure are on the order of 0.5 kJ/mol [12] and therefore not accessible with current free energy calculations for systems of this size.

F. Orientational Polarization. A possible candidate for the order parameter in the Marčelja–Radić type

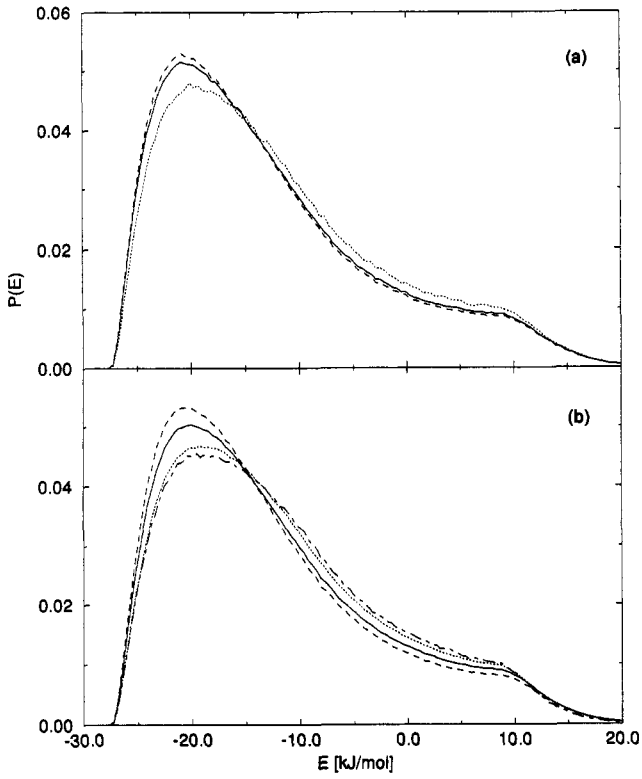

Figure 15. Distributions of pair energies: (i) full line, one molecule belongs to the first shell; (ii) dotted line, one molecule belongs to the second shell; and (iii) dashed line, both molecules belong to the first shell for (a) small liquid crystalline phase system and (b) large liquid crystalline phase system. For comparison the distribution for a bulk system at $T = 333$ K is drawn in part b (dotted–dashed line).

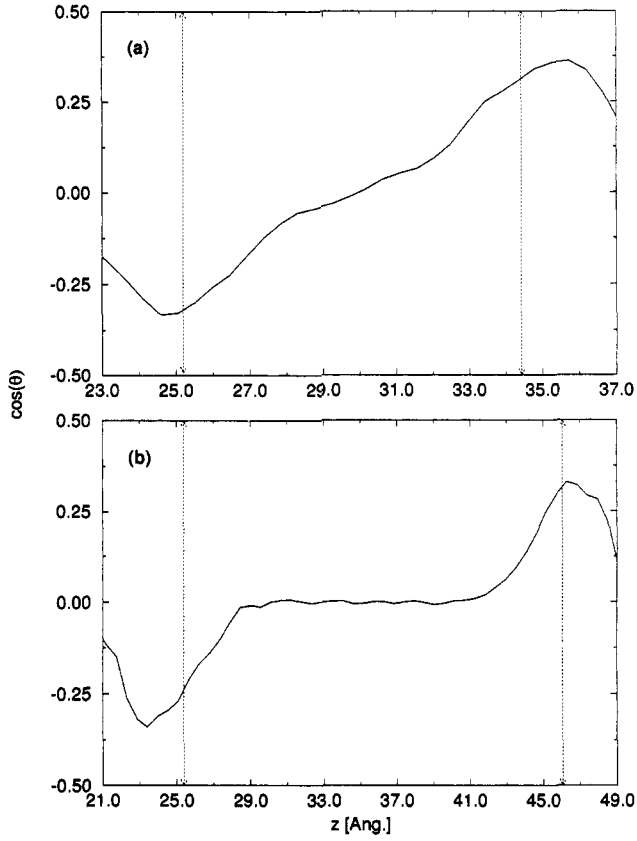

Figure 16. Orientational polarization profiles of the water molecules in the gel phase: (a) small gel phase system and (b) large gel phase system. The dotted vertical arrows indicate the lipid/water boundary as defined in the text.

theories[7-9] is the water polarization. Previous simulations showed either an oscillatory[18] or a smooth polarization profile.[12] An explanation for the differences in the two studies could be due to the fact that the hydrocarbon chains were fixed in one of the simulations.[18] This could lead to a higher degree of order in the lipid bilayer and a reduced surface roughness of the head groups. Therefore, it is possible that the increased order in the gel phase leads to a similar effect.

The orientational polarization of water molecules is defined as the average cosine angle between the water dipole and the vector in the positive z-direction. The profiles of the orientational polarization are shown in Figures 16 and 17. The polarization shows no oscillatory behavior in the liquid crystalline phase or in the gel phase. The wide distribution of the $N(CH_3)_3$ groups (see Figures 5 and 6) apparently produces a surface which is rough enough to produce a smooth polarization profile. Of special interest is the case of the large gel phase system since it contains more water than permitted under natural conditions. We see from the polarization profile that the membrane polarizes the water about 6 Å from the edge of the bilayer into the water phase. From comparison with Figure 6 we observe that the region of non-zero polarization extends only slightly beyond the region of non-zero methyl density. The water between 30 and 40 Å is essentially bulk like. This observation can also give some insight into the problem of why gel phase systems have a maximum hydration of 11 water molecules/lipid. By increasing the water content in the gel phase system from 11 to 20.5 water molecules/lipid the thickness of the water slab increases from 9.0 to 20.7 Å. The increase in the thickness of the water layer corresponds closely to the thickness of the water slab, which is not polarized by the bilayer. For the water molecules in this slab there is essentially no difference in the environment between the bulk phase and this slab. Therefore, long range attractive forces between bilayers will expel this extra water and maintain a maximum hydration of about 11 water molecules/lipid.

G. Electrostatic Potential. The head group of the DPPC molecules has a positive charge around the $N(CH_3)_3$ groups and a negative charge around the PO_4 groups (see Table 1). The small angle of inclination of the PN vectors from the membrane surface will therefore give rise to a dipolar potential. This dipolar potential will, however, produce a reorientation polarization of the water molecules which will compensate the electric field emanating from the head groups. These effects are shown in Figures 16 and 17.

The total electrostatic potential is a result of a balance between the potential due to the head groups and the potential due to the water molecules. To obtain the potential, we first have to calculate the local excess charge density $\rho(z)$ as a function of the position z. The potential can be calculated from the charge density according to

$$\psi(z) - \psi(0) = -\frac{1}{\epsilon_0}\int_0^z dz' \int_0^{z'} \rho(z'')\, dz'' \qquad (3.2)$$

The total electrostatic potential as well as the contributions of the head groups and the water for the four systems is displayed in Figures 18 and 19. (We set the potential inside the bilayer to zero.) In all four cases, the individual contributions are on the order of +2 to −4 V. In the case of the gel phase the two contributions compensate each other to give total potentials of −1.33 (small system) and −1.31 V (large system). For the liquid crystalline systems, the potential is considerably smaller: −0.69 (small system)

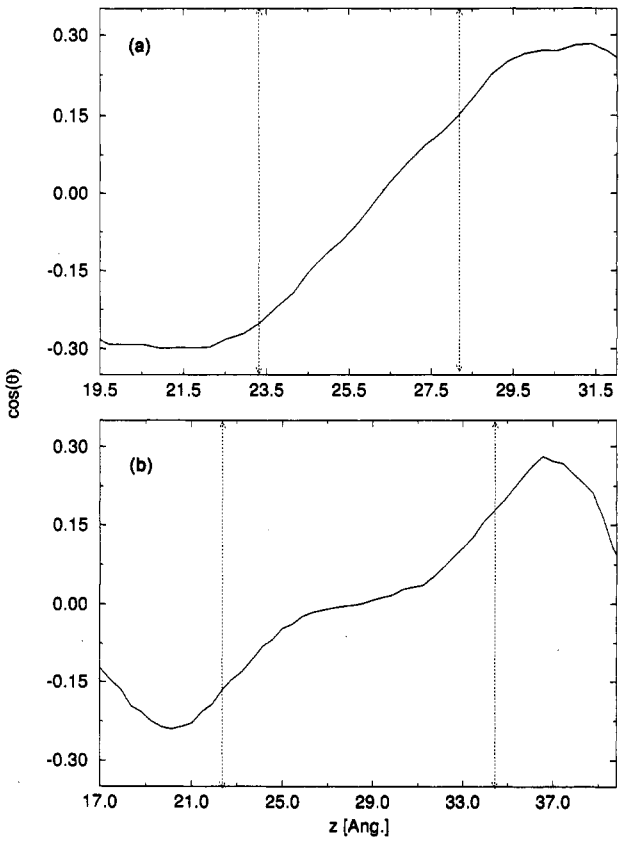

Figure 17. Orientational polarization profiles of the water molecules in the liquid crystalline phase: (a) small liquid crystalline phase system and (b) large liquid crystalline phase system. The dotted vertical arrows indicate the lipid/water boundary as defined in the text.

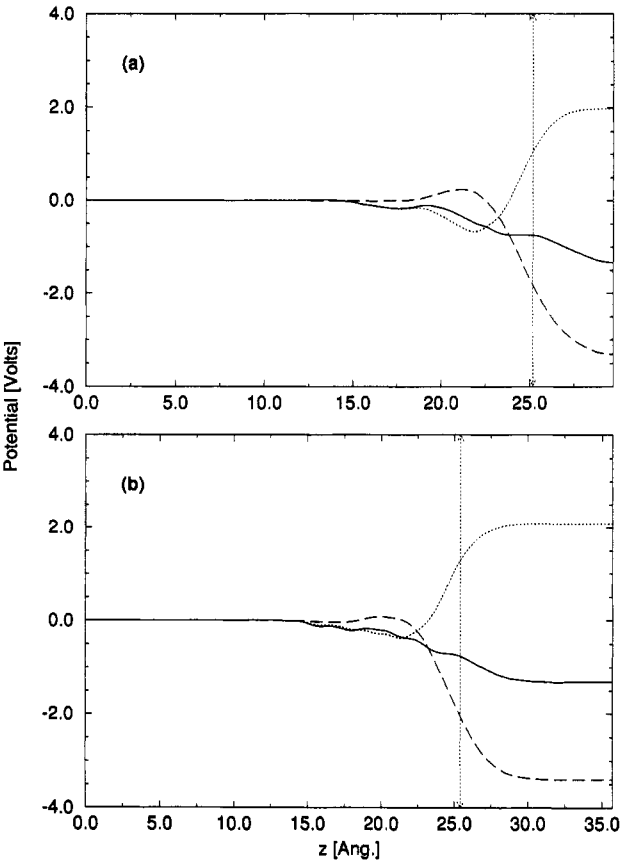

Figure 18. Electrostatic potentials for the gel phase systems: (i) dotted line, potential due to lipid molecules; (ii) dashed line, potential due to water molecules; and (iii) full line, total potential for (a) small gel phase system and (b) large gel phase system.

and −0.95 V (large system). The latter values are larger than the values reported experimentally which range between −0.2[33] and −0.4 V.[64] Note that the calculated dipole potential is larger in the gel phase than in the liquid crystalline phase, in agreement with experimental observations.[65-67] For comparison it is interesting to note that a linearized Poisson−Boltzmann approach leads to a much smaller value for DMPC of 23 mV.[68] In all cases considered here, the dipolar contributions from the water overcompensate the dipole potential from the head groups. Although the value of the total potential is larger than experimental values, it is gratifying to see that in both liquid crystalline cases the potential has the correct sign which is an improvement compared to the previous study.[12]

H. Minimum Distance between Head Groups. The atom distribution in the z-direction of Figures 5−8 gives some insight into the question of how close the head groups of opposing bilayers approach each other. However, since the distributions are rather broad and, in the case of the small liquid crystalline system, even overlapping, these figures might be misleading, because one has to keep in mind that these functions are projections onto the z-axis. Atoms with the same coordinate z might still have a large spatial separation. Therefore, we calculated here the minimal distance from a given head group to any one of the head groups of the opposing membrane. We display in Figure 20 the probability distribution $P(d_{min})$ of finding a minimum distance d_{min} between the CH_3 groups belonging to opposing head groups. (As we verified, this is virtually identical with the minimum head group−head group distance.) In the graph, the large gel phase system is omitted since the distribution starts only at distances of about 10 Å.

We observe from this graph how close the head groups approach each other. To be separated by just one layer of water molecules we estimated from Figure 13 that the CH_3 groups have to be separated by about 6.8 Å. In the STUB parameter set of AMBER 4.0 the Lennard-Jones parameter σ of a CH_3 group is 3.86 Å. That means that at close contact the two CH_3 groups are separated by about 4.3 Å ($= 2^{1/6}\sigma$). Indeed, if we look at the minimum distance distribution for the small liquid crystalline system we find a maximum at about 4.4 Å and another maximum at about 6.7 Å. We conclude that the CH_3 pairs belonging to the first peak are in close contact with each other, while the pairs belonging to the second peak are separated by just one water layer. In the small gel phase system we see a pronounced peak at about 6.9 Å, almost exactly the same distance as in the small liquid crystalline system. At distances smaller than 6.9 Å the distribution function quickly drops, and at 4 Å it has a very small value. The observation that the distribution function drops very quickly at distances below 6.9 Å shows that there is a barrier for the CH_3 groups to approach each other by less than 6.9 Å. Only if the membranes are pushed together by reducing the bilayer separation can the head groups overcome this barrier.

From the pair distribution functions in Figure 13 one can also estimate the distance between two CH_3 groups if they are separated by two water layers. The distance

(64) Pickar, A. D.; Benz, R. *J. Membr. Biol.* **1978**, *44*, 353.
(65) MacDonald, R. C.; Simon, S. A. *Proc. Natl. Acad. Sci. U.S.A.* **1987**, *84*, 4089.
(66) Simon, S. A.; McIntosh, T. J.; Magid, A. D. *J. Colloid Interface Sci.* **1988**, *126*, 74.
(67) Simon, S. A.; McIntosh, T. J. *Proc. Natl. Acad. Sci. U.S.A.* **1989**, *86*, 9263.
(68) Zheng, C.; Vanderkooi, G. *Biophys. J.* **1992**, *63*, 935.

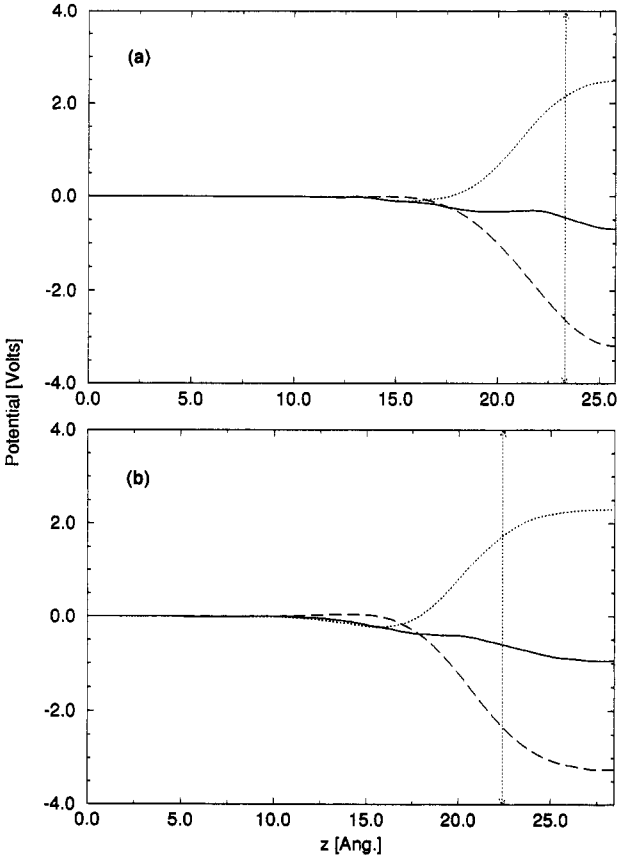

Figure 19. Electrostatic potentials for the liquid crystalline phase systems: (i) dotted line, potential due to lipid molecules; (ii) dashed line, potential due to water molecules; and (iii) full line, total potential for (a) small liquid crystalline phase system and (b) large liquid crystalline phase system.

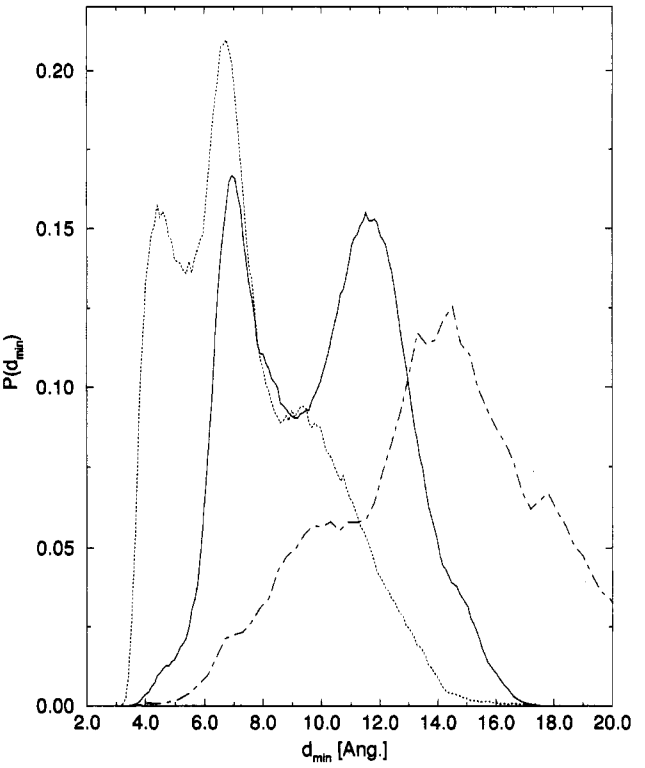

Figure 20. Minimum distances between CH_3 groups of opposing membranes: (i) full line, small gel phase system; (ii) dotted−dashed line, large liquid crystalline system; and (iii) dotted line, small liquid crystalline system.

from the CH_3 groups to their respective water layers is 3.4 Å. From experiments[69] and simulations[70] of pure water it has been found that the nearest neighbor distance between two water molecules is about 2.8 Å. The distance of two CH_3 groups separated by two water layers should therefore be 9.6 Å. Indeed, if we look at Figure 20 we find at this distance a shoulder in the distribution functions of the small and large liquid crystalline systems. In the distribution function for the small gel phase system this shoulder is not present. This function is dominated by the two prominent peaks at 6.9 and 11.6 Å. The existence of the double maximas is probably related to the splitting of the nitrogen positions as seen in parts a and d of Figure 5.

To estimate the contribution to the total hydration force from head groups in close contact and from head groups separated by one or two water layers, we would have to know the free energy between them as a function of distance. For distances close to the Lennard-Jones radius we expect a strong increase in the free energy. This has been confirmed in a model calculation of the potential of mean force between two tetramethylammonium ions.[27] Although there is only a small fraction of pairs of CH_3 groups with distances smaller than 6 Å in the small gel phase and large liquid crystalline systems, they could still contribute a substantial fraction to the hydration force.

From the electron density profiles we concluded that the bilayer separation in the small gel phase system is 9.0 Å and in the large liquid crystalline system 12.1 Å. The distribution of the minimum distances tells us, however, that in both systems, which are close to full hydration, individual head groups can come quite close to each other. This observation is confirmed by the snapshots in Figures 1 and 2. In both systems we see head groups coming quite close to each other.

IV. Discussion and Summary

The main results of this paper can be summarized as follows:

Simulations of DPPC multilayers in the liquid crystalline phase show very broad distributions of head group atoms. A similar broad distribution, but for DOPC (dioleoylphosphatidylcholine) in the liquid crystalline phase, was inferred from X-ray and neutron diffraction data by Wiener and White.[71] This indicates a very rough surface (see also the snapshot in Figure 2) which results in a smoothly decaying water density. In the liquid crystalline systems even the distribution of the carbonyl atoms, indicating the positions of the center of mass of the molecules, is rather broad. In the gel phase systems, however, the carbonyl distributions are narrower. Even the distributions of the phosphate groups are narrow, whereas the broad distributions of the $N(CH_3)_3$ groups can be attributed to the existence of two conformations of the head groups. These two conformations of the head group produce a rough surface which in turn leads to a smooth decay of the water density in the head group region.

We also observed from our simulations that the chain order parameters for the tails of the lipid molecules are in good agreement with experiments. The numbers of g,

(69) Postorino, P.; Tromp, R. H.; Ricci, M.-A.; Soper, A. K.; Neilson, G. W. *Nature* **1993**, *366*, 668.
(70) Jorgensen, W. L.; Chandrasekhar, J.; Madura, J. D.; Impey, R. W.; Klein, M. L. *J. Chem. Phys.* **1983**, *79*, 926.
(71) Wiener, M. C.; White, S. H. *Biophys. J.* **1992**, *61*, 434.
(72) Mendelsohn, R.; Senak, L. In *Biomolecular Spectroscopy*; Clark, R. J. H., Hester, R. E., Eds.; Advances in Spectroscopy; John Wiley: Chichester, 1993; Vol. 20, Part A, pp 339−380.
(73) Nagle, J. F.; Wilkinson, D. A. *Biophys. J.* **1978**, *23*, 159.

gg, or *gtg* conformations per chain are lower than in experiments; however, the experimental data show a large scatter.

The roughness of the membrane surface in the liquid crystalline as well as the gel phases leads to a smoothly decaying polarization of the water molecules. The width of the water polarization can be estimated from the gel phase simulation with 20.5 water molecules/head group. Even though the water polarization extends from the above defined boundary of the bilayer about 6 Å into the water region, we realize, however, that this definition of the bilayer boundary is rather arbitrary. Comparing the distribution of the methyl groups in Figure 6 with the polarization profile of Figure 16 we see that the water polarization does not extend beyond one layer from the furthest extension of the methyl group. In the other systems the polarization profiles decay continuously over the whole water slab.

The electrostatic potential is a result of a balance between contributions from the dipoles of the head groups and from the orientational polarization of the water molecules. We find in all cases an overcompensation of the dipole potential of the head groups by the water dipole potential leading to a net negative electrostatic potential. (The potential inside the bilayer is positive with respect to the water layer.) This observation is in agreement with experiments for liquid crystalline systems. The absolute value of the calculated total potential is, however, too large.

From the distribution of the hydrogen bond energies we find that water molecules form a distinct layer around the head groups, which may be considered as an effective extension of the head group for another 2−3 Å into the water region. This might give rise to the observed hydration force since it is plausible that the layer of water molecules with stronger hydrogen bonds forms an additional barrier for the approach of two membranes.

Another cause for the hydration force is the surprisingly small separation of the head groups of the opposing bilayers. From the distribution of the minimal distance between opposing head groups (Figure 20) we observe that (a) the distribution for the small liquid crystalline system has two maxima, one at 4.4 and the other at 6.7 Å. (b) In the small gel phase system we find a maximum at 6.9 Å, close to the corresponding value in the small liquid crystalline system. For distances smaller than 6.9 Å the distribution function quickly drops. (c) In the small and large liquid crystalline systems we find some indication for head group pairs which are separated by two water layers (corresponding distance, 9.6 Å). These observations suggest that there are two favorable sets of distances in the approach of head groups. In the first set, the head groups are separated by one or two water layers (distances, 6.8 and 9.6 Å) and in the second set the head groups are in close contact (distance, 4.3 Å). These observations confirm the conclusion from the hydrogen bond analysis that the hydration shell around the lipid head group forms a barrier in the approach of the lipid bilayers.

The hydrogen bond analysis and the minimum distance curve suggest the following picture: The surface of the membrane is very rough on a molecular length scale. Due to this roughness some head groups approach each other rather close even at water contents of, for example, 11 water molecules/head group. We also observe that the orientational ordering in the water region propagates only over short distances (not more than one layer from the furthest extension of the $N(CH_3)_3$ groups). Therefore, if the orientational polarization gives rise to the observed hydration force, this force can operate already at distances around 10 Å, because the roughness of the membrane surface brings head groups of opposing membranes into close proximity. At the same time the orientational polarization can carry the hydration force only about two water layers beyond the range of steric interactions.

Another indication that the solvation layer of water may be involved in the hydration pressure arises from the hydrogen bond analysis. Next to the membrane head groups we find a layer of water molecules with stronger hydrogen bonds. If two bilayers approach each other these layers might form a barrier. In the minimum distance distributions we find some indications which confirm this picture. Thus, for the small liquid crystalline system as well as for the small gel phase system we find a substantial fraction of head group pairs which are either in close contact or separated by just one water layer.

So far, it is difficult to assess to what extent the two effects—formation of an enhanced hydrogen bond network versus direct contact of head groups—contribute to the hydration pressure in the region from 4−5 to 8−9 Å. The hydrogen bond analysis reflects only energetic contributions to the free energy and neglects entropic contributions. Since the free energies involved in these effects are on the order of 0.5 kJ/mol we are not able to quantify the two contributions.

Acknowledgment. We thank Dr. T. Darden of NIEHS for providing the PME code, Dr. S.-J. Marrink and Professor G. Vanderkooi for providing the initial configurations, Professors S. Simon and T. McIntosh of Duke University for important discussions and providing the experimental electron density data, and L. Sremaniak and M. Lyons for carefully reading the manuscript. The simulations were performed at the North Carolina Supercomputer Center. This work was supported by the Office of Naval Research.

LA950277Q